Neutralization of IL-10 Produced by B Cells Promotes Protective Immunity during Persistent HCV Infection in Humanized Mice

Min Liu[a,#], Han-Yu Chen[a,b,#], Liang Luo[a,#], Yaping Wang[a], Dongli Zhang[a], Neng Song[c], Fu-Bing Wang[d], Qiao Li[e], Xiao-Lian Zhang[a] , Qin Pan[a,*]

Affiliations

[a]State Key Laboratory of Virology and Medical Research Institute, Hubei Province Key Laboratory of Allergy and Immunology and Department of Immunology, Wuhan University School of Basic Medical Sciences, Wuhan, 430071, China

[b]Department of Laboratory Medicine, Jingzhou Central Hospital, Jingzhou 434020, Hubei Province, China.

[c]Department of Laboratory Medicine, Hubei Provincial Hospital of Integrated Chinese&Western Medicine, Wuhan, 430015, China

[d]Department of Laboratory Medicine, Zhongnan Hospital of Wuhan University, Wuhan, 430071, China

[e]Department of Surgery, University of Michigan, Ann Arbor, MI, 48109, USA

This is the author manuscript accepted for publication and has undergone full peer review but has not been through the copyediting, typesetting, pagination and proofreading process, which may lead to differences between this version and the Version of Record. Please cite this article as doi: 10.1002/eji.201948488.

[#]These authors contributed equally to this work.

[*]Corresponding author should be addressed to Q. P.: Qin Pan (panqincn@whu.edu.cn), Department of Immunology, Wuhan University School of Medicine, Donghu Road 185#,Wuhan 430071, Hubei Province, P. R. China. Tel: 86-18627103146

Abstract

Chronic hepatitis C virus (HCV) infection can lead to cirrhosis and is associated with increased mortality. Interleukin (IL)-10-producing B cells (B10 cells) are regulatory cells that suppress cellular immune responses. Here, we aimed to determine whether HCV induces B10 cells and assess the roles of the B10 cells during HCV infection. HCV-induced B10 cells were enriched in $CD19^{hi}$ and $CD1d^{hi}CD5^{+}$ cell populations. HCV predominantly triggered the TLR2-MyD88-NF-κB and AP-1 signaling pathways to drive IL-10 production by B cells. In a humanized murine model of persistent HCV infection, to neutralize IL-10 produced by B10 cells, mice were treated with pcCD19scFv-IL-10R, which contains the genes coding the anti-CD19 single-chain variable fragment (CD19scFv) and the extracellular domain of IL-10 receptor alpha chain (sIL-10Ra). This treatment resulted in significant reduction of B10 cells in spleen and liver, increase of cytotoxic $CD8^{+}$ T cell responses against HCV, and low viral loads in infected humanized mice. Our results indicate that targeting B10 cells via neutralization of IL-10 may offer a novel strategy to enhance anti-HCV immunotherapy.

HCV predominantly triggers the TLR2-MyD88-NF-κB and AP-1 signaling pathways to drive IL-10 production by B cells. Neutralization of IL-10 produced by B10 cells promotes anti-HCV immunity in a humanized murine model of persistent HCV infection. These results provide insight into a novel immunotherapy strategy for HCV treatment.

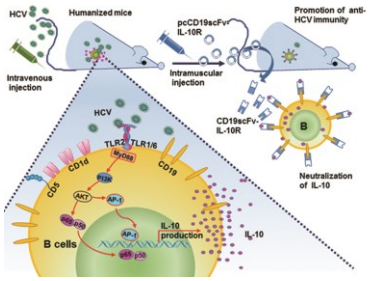

Keywords: HCV; infection; B cells; IL-10; immunotherapy

Introduction

Hepatitis C virus (HCV) is a blood−borne virus characterized by high chronic infection rates (over 80%) [1]. Although the use of direct-acting antivirals (DAAs) significantly improved the outcome of HCV treatment, these costly therapeutic cocktails already face issues such as viral mutation and reinfection following therapy [2]. Additionally, the failure to successfully manage chronic HCV infection in specific patient populations, and the lack of an effective vaccine against HCV represent major hurdles to controlling this global infection [3, 4]. Therefore, new insights into the pathogenesis of HCV and the virus-host response are needed to overcome these challenges.

HCV has evolved multiple strategies to evade host immunity and develop chronic infection in humans. Increased levels of IL-10 producing B cells (B10 cells) have been found in chronic hepatitis C (CHC) patients and is correlated with poor virus elimination, indicating that B10 cells are involved in the progress of chronic HCV infection [5]. B10 cells, a subset of regulatory B cells (Bregs), inhibit various immune responses through their IL-10 production [6]. These cells reportedly participate in viral immune evasion during infection with human immunodeficiency and hepatitis B viruses [7, 8]. However, little is known about the role of B10 cells in HCV infection.

A single-chain variable fragment (scFv) is recombinant monovalent Ab lacking the constant part of both the heavy and light chains [9, 10]. We recently employed the recombinant plasmid pcCD19scFv-IL10R, which contains the genes for anti-CD19 single-chain variable fragment (CD19scFv) and extracellular domain of IL-10 receptor alpha chain (sIL-10Ra) to specifically inhibit B cell-secreted IL-10 as well as the regulatory activity of B10 cells in a murine model [9]. In the present study, we present a novel strategy to potentially enhance anti-HCV immunotherapy via the neutralization of IL-10 secretion by B cells.

Results

HCV Induces B10 Cells in Human PBMCs in Vitro

Increased B10 cell levels have been found in CHC patients [5]; therefore, we measured the frequency of B10 cells in human PBMCs after stimulation with HCVcc. As shown in Fig. 1A

and 1B, stimulation with HCV significantly increased the percentage of IL-10^{+}CD19^{+} B cells in PBMCs compared with the control medium group (3.15 % ± 1.48 % versus 0.52 % ± 0.35 %). The histograms overlays showed that the whole peak was shifted up in HCV group, indicating that not only a subset of B cells upregulated IL-10 after exposure to HCV, but probably most of B cells (Fig. 1B). Blood B10 cells from adult humans reportedly show heightened levels of CD19 [6]; therefore, we analyzed the distribution of HCVcc-induced B10 cells in CD19^{lo} and CD19^{hi} cell populations. As shown in Fig. 1C and 1D, markedly higher frequencies of HCVcc-induced B10 cells were observed in CD19^{hi} B cells compared with CD19^{lo} B cells. These results indicated that increased B10 cell levels might be associated with HCV infection.

Murine B10 Cells Are Enriched in CD19^{hi} and CD1d^{hi} CD5^{+} Populations after HCV Stimulation in Vitro

To investigate whether HCV directly induces B cells to produce IL-10, purified murine B cells were stimulated with HCVcc in vitro. As shown in Fig. 2A, IL-10 production by CD19^{+} B cells significantly increased after HCVcc stimulation. The frequency of B10 cells in CD19^{+} B cells persistently increased upon stimulation for an extended period of time (48 h-72 h) or with increased concentrations of HCVcc (5×10^{5}-5×10^{6} RNA copies/mL; Fig. 2B, 2C and Supporting information Fig. 1A, 1B). These results demonstrated that HCVcc directly induces production of murine B10 cells in vitro. Consistent with the distribution of HCVcc-induced human B10 cells, murine B10 cell frequency was much higher in the CD19^{hi} population than in the CD19^{lo} population after HCVcc stimulation (Figure 2D). High B10 cell percentages were also found in CD1d^{hi}CD5^{+} after stimulation with HCVcc (Fig. 2E).

$CD1d^{hi}CD5^{+}$ B cells contains marginal zone (MZ) B and B1 B cells [11], which can be rapidly recruited into early adaptive immune responses in a T cell-independent manner.

HCV Drives IL-10 Production by B Cells via TLR2-MyD88-NF-κB and AP-1 Signaling pathways in Vitro

TLR2 and TLR4 signaling in immune cells can be triggered by HCV [12, 13], and is reportedly involved in IL-10 production in B cells [14, 15]. Therefore, we investigated whether TLR2 and TLR4 were involved in HCV-induced IL-10 production by B cells. IL-10 levels decreased after HCV stimulation by approximately 70 % and 50 % in $TLR2^{-/-}$ and $TLR4^{-/-}$ groups, respectively, compared with WT group (Fig. 3A). These results indicated that HCV-induced IL-10 production by B cells was both TLR2 and TLR4 dependent, predominantly via the TLR2 signaling pathway.

We then explore the adapter proteins and transcription factors downstream of TLR2 that significantly contributed to IL-10 production. As shown in Figure 3B, inhibition of MyD88, P38, PI3K, NF-κB, and AP1 significantly decreased IL-10 production by HCVcc-treated B cells. Immunoblot analysis revealed that PI3K and its downstream target AKT were highly phosphorylated after 15 min of HCV stimulation (Fig. 3C and Supporting information Fig. 2A). The peaks of NF-κB (p-P65) and AP-1 (p-c-fos) activation were obtained after 15 min and 2 h of HCV stimulation, respectively (Fig. 3C and Supporting information Fig. 2A). Compared with WT B + HCVcc group, HCV-induced activation of PI3K, AKT, NF-kB and AP-1 in B cells was significantly reduced in the $TLR2^{-/-}$ group, (Fig. 3D and Supporting informaation Fig. 2B) or in the presence of MyD88 inhibitor (Fig. 3E and Supporting

information Fig. 2C). These results further demonstrated that HCVcc triggers the TLR2-MyD88-NF-κB and AP-1 signaling pathways in B cells.

Neutralization of IL-10 Secretion by B cells Reduces Viral Loads during Persistent HCV Infection

Transgenic mice harboring both human CD81 and OCLN (occludin) genes have been reportedly used as an animal model of persistent HCV infection at a chronicity rate comparable to humans [16, 17]. Human SRBI (scavenger receptor class B type I) and CLDN1 (claudin1) are reportedly both required for HCV entry into hepatocytes [18-20]. In the present study, ICR^{Tg4R+} humanized mice that express human CD81, OCLN, SRBI and CLDN1 molecules in the liver were used as a persistent HCV infection mode. As shown in Supporting information Fig. 3A and 3B, 1345 ± 134 HCV RNA copies/mL in serum, and HCV NS3 and core proteins in the liver tissues were detected in the ICR^{Tg4R+} mice 60 d post infection (dpi), demonstrating that HCV established persistent infection in the ICR^{Tg4R+} mice.

In the present study, we used pcCD19scFv-IL-10R to investigate the role of B10 cells during the HCV infection in vivo. On Day 0, ICR^{Tg4R+} mice were infected (i.v.) with HCVcc. pcCD19scFv-IL-10R and pcIL-10R were injected (i.m.) into the mice weekly (Fig. 4A). Soluble CD19scFv-IL-10R and sIL-10Ra proteins were detected in the serum 5 d post plasmid injection (Supporting information Fig. 4A). On Day 60, IL-10 levels were significantly decreased in the pcCD19scFv, pcCD19scFv-IL-10R and pcIL-10R groups, indicating that CD19scFv, CD19scFv-IL-10R and sIL-10Ra proteins effectively decreased serum IL-10 in mice (Fig. 4B). Treatment with pcCD19scFv-IL-10R and pcIL-10R also

significantly decreased the HCV load in the mice compared with the pcDNA group, but treatment with pcCD19scFv slightly reduced the HCV load in the mice (Fig. 4C).

Consistent with decreased HCV loads, decreased NS3 expression was observed in liver tissues of pcCD19scFv-IL-10R and pcIL-10R groups (Figure 4D and Supporting information Fig. 4B). Treatment with pcCD19scFv-IL-10R and pcIL-10R markedly reduced hepatocellular swelling and periportal sinusoidal fibrosis (Fig. 4E and Supporting information Fig. 4C). Together, these results demonstrated that pcCD19scFv-IL-10R and pcIL-10R treatments inhibit HCV infection in vivo.

Blocking IL-10 Production by B Cells Reduces B10 Cells in HCV-Infected Mice

To address the effects of pcCD19scFv-IL-10R treatment on B10 in vivo, we examined B10 cells in HCV-infected mice. Both pcCD19scFv-IL-10R and pcIL-10R treatments significantly reduced the frequency of splenic B10 cells (Fig. 5A and Supporting information Fig. 5A). In immunofluorescence assay, IL-$10^{+}$$CD19^{+}$ B cells were found in $CD19^{+}$ B cells accumulated in the liver tissues of HCV and pcDNA+HCV groups, while reduced B10 cells were observed in the liver tissues of pcCD19scFv-IL-10R and pcIL-10R groups (Fig. 5B). These results indicated that pcCD19scFv-IL-10R treatment might hinder B10 cell function via neutralization of IL-10 and reduction of HCV-induced B10 cells (Fig. 5A and 5B). All mice (including the pcDNA group) subjected to plasmid injection showed a decreased frequency of splenic Tregs (Fig. 5C and Supporting information Fig. 5B).

Blockage of IL-10 Secretion by B10 Cells Enhances CD8$^+$T Cytotoxicity in HCV-Infected Mice

To further evaluate the anti-HCV immune effect in mice after pcCD19scFv-IL-10R treatment, we determined the frequencies of Th1, Th2 and Th17 cells by detecting IFNγ, IL-4 and IL-17A respectively (Fig. 6A-6C and Supporting information Fig. 6A-6C). No obvious differences were observed in frequencies of Th1, Th2 and Th17 cells among the groups, indicating that neutralizing B cell-produced IL-10 nearly had no influence on Th polarization during HCV infection. However, the percentages of perforin$^+$CD8$^+$T cells from the spleen and liver in pcCD19scFv-IL-10R and pcIL-10R groups were significantly higher than that in pcCD19scFv and pcDNA groups, indicating that number of cytotoxic CD8$^+$ T cells could be enhanced in pcCD19scFv-IL-10R and pcIL-10R groups (Fig. 7A-7B and Supporting information Fig. 7A-7B).

We then examined the cytotoxicity of the splenocytes using an LDH assay. The highest level of splenocyte cytotoxic activity was observed in pcCD19scFv-IL-10R group (Fig. 7C). More importantly, at lower E:T ratios of 5:1, the splenocytes in pcCD19scFv-IL-10R group showed more effective cytotoxic activity on target cells compared with IL-10R group (Fig. 7C). These results indicated that pcCD19scFv-IL-10R treatment increases the splenocyte cytotoxicity against the HCV-infected hepatocytes. Together, our results demonstrated that treatment with pcCD19scFv-IL-10R increases CD8$^+$ T cell responses and cytotoxic activity in vivo.

Discussion

HCV is a major hepatotropic virus causing chronic hepatitis and also a ~~lymphotropic~~ virus that directly modulate B- and T cell function [21, 22]. The increased level of B10 cells in CHC patients highlights the immunomodulatory function of B10 cells during HCV infection [5]. In the present study, we found that HCV induces both human and murine B cells to produce IL-10 in vitro (Fig. 1A-1D, 2A-2E and Supporting information Fig. 1A-1B). We also found that HCV-induced murine B10 cells were enriched in $CD19^{hi}$ and $CD1d^{hi}CD5^{+}$ cell populations (Fig. 1C, 1D, 2D and 2E). This finding was consistent with previous studies which demonstrated that murine B10 cells are predominantly contained within a $CD1d^{hi}CD5^{+}$ B cell subpopulation upon stimulation with lipopolysaccharides (LPS) [23].

HCVcc does not infect PBMCs [24], but HCV virus and its viral antigens can stimulate B cells. HCV core protein is reportedly recognized by TLR2 [12, 25]. High concentrations of virion-free soluble core protein are readily detected in the plasma of HCV-infected individuals [26]. In the current study, HCV induced B10 cells mainly via TLR2 signaling pathway (Fig. 3A, 3B and 3D). Therefore, we speculated that soluble HCV core proteins can be released from HCVcc-infected cells, which might be involved in induction of B10 cells. Moreover, production of IL-10 in $TLR4^{-/-}$ B cells was reduced compared with WT B cells after HCV stimulation, indicating that TLR4 signaling might be involved in IL-10 production in B cells (Fig. 3A). It has been reported that HCVcc binds to B cells via other receptors like CD81, SRBI, dendritic cell-specific intercellular adhesion molecule-3-grabbing non-integrin (DC-SIGN) and L-SIGN [27]. Whether TLR4 and other receptors are involved in induction of HCV-induced B10 cells should be demonstrated in future work.

All mice (including the pcDNA group) subjected to plasmid injection showed decreased Tregs, indicating that DNA plasmid might act as an adjuvant and reduce Tregs during HCV

infection (Fig. 5C and Supporting information Fig. 5B). These results also demonstrated that experimental procedure alone affected the immune response, and the effect of pcCD19scFv-IL-10R and pcIL-10R treatment on Tregs was limited (Fig. 5C and Supporting information Fig. 5B).

CD19-generated signals are critical for B10 cell development [23, 28]. In the current study, pcCD19scFv treatment blocked the CD19 signaling, resulting to reducing the B10 cells in HCV-infected mice (Fig. 5A, 5B and Supporting information Fig. 5A). Moreover, IL-10 acts in an autocrine manner to regulate the differentiation of B cells [29, 30]. CD19scFv-IL-10R and IL-10R might block IL-10 to bind to the IL-10 receptor on B cells, resulting to further reduction of B10 cells (Fig. 5A, 5B and Supporting information Fig. 5A).

CD19scFv has no Fc fragment. Although CD19scFv binds to CD19, it cannot mediate antibody-dependent cellular cytotoxicity (ADCC) or other cytotoxic effects via Fc fragment. In our study, the B10 cells even B cells were markedly reduced in liver tissues in the mice subjected to pcCD19scFv treatment compared with pcDNA+HCV group (Fig. 5B). Other studies show that persistent virus infections are associated with B cell dysregulations, and CHC patients ~~with~~ have the risk to develop mixed cryoglobulinemia which is associated with B-cell proliferative disorder and B-cell non-Hodgkin's lymphoma (B-NHL) [31-33]. We speculated that CD19scFv might inhibit B-cell proliferative disorder caused by chronic HCV infection. Whether the CD19 scFv inhibits of B-cell proliferative disorder or directly depletes B cells should be assessed in future work.

B10 cells reportedly skew $CD4^+$ Th cell differentiation and suppress cytotoxic $CD8^+$ T cells [34]. However, in this study, blocking IL-10 production of B cells with pcCD19scFv-IL-10R demonstrated its limited effects on Th polarization (Fig. 6A-6C and Supporting information Fig. 6A-6C). Two factors might contribute to these results: first,

pcCD19scFv-IL-10R treatment only partially neutralized IL-10 from B cells; and second, HCV-induced B10 cells would be functionally heterogeneous resulting in the limited effects on Th polarization. Nevertheless, pcCD19scFv-IL-10R treatment markedly increased perforin production by $CD8^+$ T cells and promoted the cytotoxicity of splenocytes against HCV-infected cells (Fig. 7A-7C and Supporting information Fig. 7A-7B), demonstrating that neutralization of B cell-secreted IL-10 could promote cytolytic activity of $CD8^+$T cells against HCV. However, titers of HCV were not reduced in pcCD19scFv group, while IL-10 level and B10 cells were decreased in pcCD19scFv group compared pcDNA control group (Fig. 4B, 4C and 5A). These indicated that other mechanisms beyond B10 cell reduction or even IL-10 reduction might be involved in decreasing HCV titer in pcIL-10R and pcCD19scFv-IL-10R groups.

There are some limitations in our current study. The mock control of supernatants from non-infected Huh7.5.1 cells should be used to exclude the effect of possible contaminates in the HCVcc preparation. It is better to use anti-CD20 or anti-B220 antibody to detect B cells in the murine model to exclude the possibility that the binding capacity of anti-CD19 antibody influenced by CD19scFv. The levels of IL-10 and plasmid encoded proteins should be measured at the same day in murine model to rule out any confounding effects of proteins on production/stability of plasmid encoded proteins. We did not measure the inflammatory details in livers except haematoxylin & eosin (HE) analysis (Fig. 4E) in the murine model. The alanine aminotransferase (ALT) levels and more liver histology analysis should be done to evaluate the inflammatory of liver after pcCD19scFv-IL-10R or pcIL-10R treatment. Additionally, whether CD19scFv-IL10R strictly binds to B cells and whether it also neutralizes IL-10 independent of binding to CD19 need to be verified. An IL-10 knockout or even a B cell-specific IL-10 knockout mouse model needs to be employed to further clarify

the roles of B10 cells during long-term HCV infection. We will do these work in our future study.

DAAs have revolutionized HCV treatment, proving to be effective treatment options for HCV-infected individuals [35, 36]. However, the emergence of drug resistant HCV variants has been reported [37]. In our study, we showed that blocking B10 cells by treatment with pcCD19scFv-IL-10R during persistent HCV infection promotes protective immunity and alleviates liver damage caused by HCV infection by decreasing B10 cells and promoting the cytotoxicity of $CD8^+$T cells against HCV in HCV-infected humanized mice. These results indicate that B10 cells can serve as a target for HCV therapy, and immunomodulatory agents blocking B10 cell activity might be potentially effective for combination therapy against HCV infections.

Materials and methods

Blood Samples

14 healthy donors from Hubei Provincial Hospital of Integrated Chinese&Western Medicine (Wuhan, China) were provided informed consent before blood donation. Peripheral blood mononuclear cells (PBMCs) were obtained by Ficoll density gradient centrifugation (Axis-Shield, Dundee, Scotland). This study was approved by the ethics committee of the Wuhan University School of Basic Medical Science (No.150001).

Animals

Animal protocols were approved by the Institutional Animal Care and Use Committee of the Animal Laboratory Center of Wuhan University (No. 2017077 and No. 2017095). Wide type (WT) C57BL/6, TLR2$^{-/-}$ and TLR4$^{-/-}$ mice were purchased from the Biomedical Research Institute of Nanjing University (Nanjing, China). ICR^{Tg4R+} humanized mice expressing human CD81, OCLN, SRB1 and CLDN1 genes in liver tissues, were bred on an ICR genetic background and characterized by Beijing Vitalstar Biotechnology Co., Ltd (Beijing, China). All mice were bred and maintained at the university animal facility under standard specific-pathogen free conditions.

Plasmids, Virus and Cell Culture

pcCD19scFv-IL-10R, pcIL-10R and pcCD19scFv were constructed as previously described [9]. Huh7.5.1 cells were cultured in complete Dulbecco's modified Eagle's medium (DMEM, Thermo Fisher Scientific, Waltham, USA) with 10% foetal bovine serum (FBS, HyClone, Logan, USA). Expansion of cell culture-derived HCV (HCVcc, genotype 2a, Japanese fulminant hepatitis 1, JFH1 isolate) was performed using Huh7.5.1 cells as described in our previous publication [38]. In brief, Huh7.5.1 cells were infected with HCVcc (multiplicity of infection (MOI) of ~1; 1×10^7 RNA copies/mL). The supernatants from infected cells were harvested after 5 d and filtered through a 0.22-μm filter, concentrated 100-fold using an Amicon Ultra-4 (Millipore, Burlington, USA) at 4000 g for 45 min and aliquoted for storage at −80 °C.

Magnetic Activated Cell Sorting (MACS)

B cells were purified and isolated from murine splenocytes using CD19 positive magnetic activated cell sorting (Miltenyi Biotec, Bergisch Gladbach, Germany). Briefly, mouse splenocytes were incubated with microbeads-conjugated monoclonal rat anti-mouse CD19 antibodies at 4 ºC for 15 min. After immobilization of all these cells with a magnet, untouched CD19-cells were discharged. $CD19^+$ B cells were then flushed from the column.

Flow Cytometry (FCM)

Flow cytometry analyses were performed according to the guidelines used for immunological studies [39]. To detect human B10 cells, PBMCs (2×10^6 cells/mL) were stimulated with HCVcc (1×10^6 RNA copies/mL) in medium containing IL-2 (30 U/mL; Peprotech , Rocky Hill, USA) for 48 h. Brefeldin A (1000×) was added 6 h before harvesting the cells. Samples were harvested and incubated with human Fc Receptor Blocking Solution (Biolegend, San Diego, USA) to block FcRs, followed by staining with FITC anti-CD19 (SJ25C1). Cells were then with fixation/permeabilization buffer (Biolegend). Permeabilized cells were stained with anti-IL-10 (JES3-9D7) and isotype control APC Rat IgG1, κ Isotype (RTK2071) antibodies. In the medium group, PBMCs were cultured in the presence of IL-2 in DMEM supplemented with 10 % FBS.

To detect murine B10 cells, splenic B cells (2×10^6 cells/mL) were stimulated in vitro with various concentrations of HCVcc in medium containing IL-2 for 0-72 h. Anti-mouse CD16/CD32 antibody (clone 93) was used to block FcRs. Samples were stained with the following antibodies: FITC anti-CD19 (6D5), PerCP-Cy5.5 anti-mouse CD1d (CD1.1, Ly-38), Alexa Fluor 647 anti-CD5 (53-7.3), PE anti-IL-10 antibody (JES5-16E3) or isotype control PE Rat IgG2b, κ antibodies. In the medium group, the cells were cultured in the presence of IL-2 in DMEM supplemented with 10 % FBS.

For the murine model of HCV infection, splenocytes isolated from HCV-infected mice were directly stained with antibodies. The following antibodies were used: APC-anti-CD3(17A2), PE/Cy5/FITC-anti-CD4 (RM4-5), PerCP-Cy5.5-anti-CD8a (53-6.7), PE-anti-IFN-γ (XMG1.2), PE-anti-IL-4 (11B11), PE-anti-IL-17A (TC11-18H10.1), PE-anti-perforin (S16009A) and Alexa Fluor 488-anti-Foxp3 (MF-14). All the antibodies were purchased from Biolegend. Samples were measured using a BD FACSAria™ III flow cytometer (BD Biosciences, San Jose, USA) at the Medical Structural Biology Research Center of Wuhan University.

Enzyme-Linked Immunosorbent Assay (ELISA)

For IL-10 detection, murine splenic $CD19^+$ B cells (1×10^6 cells/mL) were stimulated with HCVcc (1×10^6 RNA copies/mL) in medium containing IL-2 for 0-72 h. IL-10 production in the supernatant was detected by ELISA (Dakewe Biotech Co., Guangdong, China). To assess the signaling adaptors involved in IL-10 production by B cells, B cells were pretreated with LY294002 (phosphoinositide-3 kinase (PI3K) inhibitor, 20 μM; Selleck, Houston, USA),

LY2228820 (P38 inhibitor, 10 μM; MedChemExpress, Monmouth Junction, USA), ST-2825 (MyD88 inhibitor, 10 μM; MedChemExpress), curcumin (activator protein 1 (AP1) inhibitor, 10 μM; MedChemExpress) or BAY 11-7082 (NF-κB inhibitor, 10 μM; Selleck) for 1 h before stimulation with HCVcc.

For the murine model of HCV infection, mouse serum was collected for IL-10 detection.

Immunoblot Analysis

B cells (1×10^6 cells/mL) were stimulated with HCVcc (1×10^6 RNA copies/mL) in medium containing IL-2 for 0-12 h. The cells were lysed in 250 μL of RIPA Lysis Buffer (Beyotime Biotechnology, Shanghai, China). Lysates were separated on a 5-10 % SDS-polyacrylamide gel, transferred onto polyvinylidene difluoride membranes (Millipore), and then probed with specific antibodies. Bound antibodies were detected with HRP-conjugated secondary antibodies and visualized by chemiluminescence (Dalian Meilun Biology Biotechnology Co., Ltd., Dalian, China). Semi-quantification was performed by densitometry using the UVP bioimaging system (UVP, Cambridge, UK). The following antibodies were used: p-PI3K p85 (Tyr607), PI3 Kinase p110α, p-AKT (Ser473), AKT (pan), p-NF-κB p65 (Ser 536), NF-κB p65, AP-1(p-c-fos) (Ser32) and β-actin antibodies. p-PI3K p85 (Tyr607) was purchased from Abcam (Cambridge, UK) other antibodies were purchased from Cell Signaling Technology (Danvers, USA).

In the murine model, mouse serum was collected 5 d after plasmid injection. Serum protein levels of CD19scFv-IL-10R, sIL-10Ra and CD19scFv were detected by immunoblotting using anti-IL-10R (R&D Systems, Minneapolis, USA) or anti-His-Tag antibody (Proteintech,

Rosemont, USA). Sixty days after HCV infection, mouse liver tissue was homogenised and analyzed by immunoblot analysis using anti-core (Abcam,), anti-NS3 (Abcam) and anti-GAPDH antibodies (ABclonal Technology, Woburn, USA).

Humanized Murine Model of Persistent HCV Infection

We developed the reported murine model for persistent HCV infection [16-18]. Briefly, 10-week-old ICR^{Tg4R+} mice were randomly divided into 6 groups (6 mice/group). On Day 0, mice were intravenously (i.v.) injected with HCVcc (MOI of ~1; 1×10^7 RNA copies/mouse). Mice were injected intramuscularly (i.m.) weekly with pcCD19scFv-IL-10R, pcIL-10R or pcCD19scFv (35 μg/100μL of phosphate buffered saline per mouse) by electroporation with an Electric Square Porator (TERESA, Shanghai, China) [9]. Electroporation was performed using 6×1 Hz pulses of 60 V/cm, with 50 ms duration and 1 s apart.

The mice were sacrificed by carbon dioxide anesthesia and cervical dislocation on Day 60. HCV RNA copies in serum were determined by reverse transcription quantitative PCR (RT-qPCR). Serum IL-10 levels were determined by ELISA. Frequencies of B10 cells and Tregs in spleens, IFN-γ, IL-4 and IL-17A production by splenic $CD4^+$ T cells, and perforin production by $CD8^+$ T cells were analyzed directly ex vivo by FCM. Cytotoxicity of splenocytes against HCV-infected hepatocytes was measured by LDH cytotoxicity assay.

RT-qPCR

HCV RNA in serum from HCVcc-infected mice was quantified using a PCR-Fluorescence Quantification Kit for HCV RNA (DaAN Gene Co., Ltd., Guangzhou, China). Briefly, HCV RNA from serum was isolated by a column containing a special silicon membrane to isolate RNA fragments. Isolated RNA samples were then subjected to RT-qPCR assay using primers provided by the manufacturer.

Histopathology, Immunohistochemistry (IHC) and Immunofluorescence

Liver tissues were fixed in 4 % paraformaldehyde, embedded in paraffin and sectioned (5 μm) for HE and Masson's trichrome staining. The IHC assay were performed as described elsewhere [16, 40] using primary antibody anti-NS3 (Abcam) and peroxidase-labelled rabbit anti-mouse IgG (Servicebio, Woburn, USA). Immunofluorescence staining was performed as described previously [39]; frozen sections of liver tissue (4 μm) were fixed and blocked, and then stained with anti-CD19 (Servicebio) and anti-IL-10 antibody (Absin Bioscience Inc., Shanghai, China). Thereafter, nuclei were stained with 4',6-diamidino-2-phenylindole (DAPI; Servicebio).

Cytotoxicity Assay

The CytoTox 96 LDH release assay (Promega, Madison, USA) was used to detect splenocyte cytotoxicity. Sixty days after infection with HCV, murine splenocytes were collected, stimulated with anti-CD3 mAb (5 μg/μL; Biolegend), anti-CD28 (2 μg/μL; Biolegend) and

IL-2 (50 IU/mL) for 5 d and used as effector cells. Hepatocytes from HCV-infected mice (HCV group) were used as target cells (10,000 cells/well) and coincubated with the splenocytes at effector to target cell ratios (E:T ratios) of 1:1, 5:1, and 10:1. After 8 h of incubation, 50 μL supernatant from each well was mixed with 50 μL of the substrate at room temperature in the dark for 15–30 min. Absorbance of samples was then measured at 490 nm to determine the LDH activity in the supernatants.

Quantification and statistical analysis

Data are presented as mean ± SD and analyzed by GraphPad Prism V 5.00 for Windows (GraphPad Software, La Jolla, USA). Statistical significance was determined by Student's t-test or ANOVA followed by Newman-Keuls post hoc test. *P*-values less than 0.05 were considered statistically significant.

Conflicts of interest

The authors declare that there is no commercial or financial conflict of interest.

Acknowledgments

This work was supported by grants from the National Key R&D Program of China (2018YFA0507603), National Science and Technology Major Project (2017ZX10201301-006, 2012ZX10003002-015), the National Natural Science Foundation of China (81971908, 31770145, 81501377, 31370197 and 21572173), the National Outstanding

Youth Foundation of China (81025008), the Major Projects of Technological Innovation of Hubei Province (2016ACA150), the Natural Science Foundation Key Project of Hubei Province (2016CFA062), and the Outstanding Youth Foundation of Hubei Province (2018CFA037). CAMS Innovation Funding For Medical Sciences (2016-I2M-2-006 and 2016-I2M-1-013), Medical Science Advancement Program (Basical Medical Sciences) of Wuhan University (TFJC 2018002) and The Fundamental Research Funds for the Central Universities (2042019kf0196).

References

1. **Ferrari, S. M., Fallahi, P., Ruffilli, I., Elia, G., Ragusa, F., Paparo, S. R., Patrizio, A. et al.**, Immunomodulation of CXCL10 secretion by hepatitis C virus: could CXCL10 be a prognostic marker of chronic hepatitis C? *J. Immunol. Res.* 2019. **2019**: 5878960.

2. **Negash, A. A., Olson, R. M., Griffin, S. and Gale, M. Jr.**, Modulation of calcium signaling pathway by hepatitis C virus core protein stimulates NLRP3 inflammasome activation. *PLoS. Pathog.* 2019. **15**: e1007593.

3. **Dhiman, R. K., Grover, G. S. and Premkumar, M.**, Hepatitis C elimination: a public health perspective. *Curr. Treat. Options. Gastroenterol.* 2019. **17**: 367-377.

4. **Heffernan, A., Cooke, G. S., Nayagam, S. Thursz, M. and Hallett, T. B.**,. Scaling up prevention and treatment towards the elimination of hepatitis C: a global mathematical model. *Lancet.* 2019. **393**: 1319-1329.

5. **Wang, L., Qiu, J., Yu, L., Hu, X., Zhao, P. and Jiang, Y.**, Increased numbers of $CD5^+CD19^+CD1d^{high}IL\text{-}10^+$ Bregs, $CD4^+Foxp3^+$ Tregs, $CD4^+CXCR5^+Foxp3^+$ follicular regulatory T (TFR) cells in CHB or CHC patients. *J. Transl. Med.* 2014. **12**: 251.

6. **Lykken, J. M., Candando, K. M. and Tedder, T. F.,** Regulatory B10 cell development and function. *Int. Immunol.* 2015. **27**: 471-477.

7. **Liu, J., Zhan, W., Kim, C. J., Clayton, K., Zhao, H., Lee, E., Cao, J. C. et al.**, IL-10-producing B cells are induced early in HIV-1 infection and suppress HIV-1-specific T cell responses. *PLoS. One.* 2014. **9**: e89236.

8. **Das, A., Ellis, G., Pallant, C., Lopes, A. R., Khanna, P., Peppa, D., Chen, A. et al.**, IL-10-producing regulatory B cells in the pathogenesis of chronic hepatitis B virus infection. *J. Immunol.* 2012. **189**: 3925-3935.

9. **Zhao, R., Liu, M., Li, X., Chen, H., Deng, J., Huang, C., Zhang, X. L. et al.**, A strategy of targeting B10cell by CD19scFv-IL10R for tumor therapy. *Biochem. Biophys. Res. Commun.* 2018. **506**: 990-996.

10. **Ma, Y., Xiang, D., Sun, J., Ding, C., Liu, M., Hu, X. , Li, G. et al.**, Targeting of antigens to B lymphocytes via CD19 as a means for tumor vaccine development. *J. Immunol.* 2013. **190**: 5588-5599.

11. **Yanaba, K., Bouaziz, J. D., Haas, K. M., Poe, J. C., Fujimoto, M. and Tedder, T. F.**, A regulatory B cell subset with a unique $CD1d^{hi}CD5^+$ phenotype controls T cell-dependent inflammatory responses. *Immunity.* 2008. **28**: 639-650.

12. **Chung, H., Watanabe, T., Kudo, M. and Chiba, T.**, Hepatitis C virus core protein induces homotolerance and cross-tolerance to Toll-like receptor ligands by activation of Toll-like receptor 2. *J. Infect. Dis.* 2010. **202**: 853-861.

13. **Imran, M., Waheed, Y., Manzoor, S., Bilal, M., Ashraf, W., Ali, M. and Ashraf, M.**, Interaction of Hepatitis C virus proteins with pattern recognition receptors. *Virol. J.* 2012. **9**: 126.

14. **Pore, D., Matsui, K., Parameswaran, N. and Gupta, N.**, Cutting edge: ezrin regulates inflammation by limiting B cell il-10 production. *J. Immunol.* 2016. **196**: 558-562.

15. **Yuan, C., Qu, Z. L., Tang, X. L., Liu, Q., Luo, W., Huang, C., Pan, Q. et al.**, *Mycobacterium tuberculosis* mannose-capped lipoarabinomannan induces IL-10-producing b cells and hinders CD4(+)Th1 immunity. *iScience.* 2019. **11:** 13-30.

16. **Chen, J., Zhao, Y., Zhang, C., Chen, H., Feng, J., Chi, X., Pan, Y. et al.**, Persistent hepatitis C virus infections and hepatopathological manifestations in immune-competent humanized mice. *Cell. Res.* 2014. **24:** 1050-1066.

17. **Chen, J., Wang, N., Dong, M., Guo, M., Zhao, Y., Zhuo, Z., Zhang, C. et al.**, The metabolic regulator histone deacetylase 9 contributes to glucose homeostasis abnormality induced by hepatitis C virus infection. *Diabetes.* 2015. **64**: 4088-4098.

18. **Qian, X. J., Zhang, X. L., Zhao, P., Jin, Y. S., Chen, H. S., Xu, Q. Q., Ren, H. et al.**, A schisandra-derived compound schizandronic acid inhibits entry of pan-HCV genotypes into human hepatocytes. *Sci. Rep.* 2016. **6**: 27268.

19. **Gerold, G., Moeller, R. and Pietschmann, T.**, Hepatitis C virus entry: protein interactions and fusion determinants governing productive hepatocyte invasion. *Cold. Spring. Harb. Perspect. Med.* 2019 DOI 10.1101/cshperspect.a036830.

20. **Regeard, M., Trotard, M., Lepere, C., Gripon, P. and Le Seyec J.**, Entry of pseudotyped hepatitis C virus into primary human hepatocytes depends on the scavenger class B type I receptor. *J. Viral. Hepat.* 2008. **15**: 865-870.

21. Russi, S., Vincenti, A., Vinella, A., Mariggio, M. A., Pavone, F., Dammacco, F. and Lauletta, G., CD5/CD20 expression on circulating B cells in HCV-related chronic hepatitis and mixed cryoglobulinemia. *Eur. J. Intern. Med.* 2019. **66**: 48-56.

22. Saadoun, D., Landau, D. A., Calabrese, L. H. and Cacoub, P. P., Hepatitis C-associated mixed cryoglobulinaemia: a crossroad between autoimmunity and lymphoproliferation. *Rheumatology (Oxford).* 2007. **46**: 1234-1242.

23. Yanaba, K., Bouaziz, J. D., Matsushita, T., Tsubata, T. and Tedder, T. F., The development and function of regulatory B cells expressing IL-10 (B10 cells) requires antigen receptor diversity and TLR signals. *J. Immunol.* 2009. **182**: 7459-7472.

24. Marukian, S., Jones, C. T., Andrus, L., Evans, M. J., Ritola, K. D., Charles, E. D., Rice, C. M. et al., Cell culture-produced hepatitis C virus does not infect peripheral blood mononuclear cells. *Hepatology.* 2008. **48:** 1843-1850.

25. Chang, S., Dolganiuc, A. and Szabo, G., Toll-like receptors 1 and 6 are involved in TLR2-mediated macrophage activation by hepatitis C virus core and NS3 proteins. *J. Leukoc. Biol.* 2007. **82**: 479-487.

26. Hu, K. Q. and Cui, W., A highly specific and sensitive hepatitis C virus antigen enzyme immunoassay for One-step diagnosis of viremic hepatitis C virus infection. *Hepatology.* 2016. **64**: 415-424.

27. Stamataki, Z., Shannon-Lowe, C., Shaw, J., Mutimer, D., Rickinson, A. B., Gordon, J., Adams, D. H. et al., Hepatitis C virus association with peripheral blood B lymphocytes potentiates viral infection of liver-derived hepatoma cells. *Blood.* 2009. **113**: 585-593.

28. Watanabe, R., Ishiura, N., Nakashima, H., Kuwano, Y., Okochi, H., Tamaki, K., Sato, S. et al., Regulatory B cells (B10 cells) have a suppressive role in murine lupus:

CD19 and B10 cell deficiency exacerbates systemic autoimmunity. *J. Immunol.* 2010. **184**: 4801-4809.

29. **Figueiro, F., Muller, L., Funk, S., Jackson, E. K., Battastini, A. M. and Whiteside, T. L.**, Phenotypic and functional characteristics of CD39(high) human regulatory B cells (Breg). *Oncoimmunology.* 2016. **5**: e1082703.

30. **Heine, G., Drozdenko, G., Grun, J. R., Chang, H. D., Radbruch, A. and Worm, M.**, Autocrine IL-10 promotes human B-cell differentiation into IgM- or IgG-secreting plasmablasts. *Eur. J. Immunol.* 2014. **44**: 1615-1621.

31. **Greczmiel, U., Krautler, N. J., Borsa, M., Pedrioli, A., Bartsch, I., Richter, K., Agnellini, P. et al.**, LCMV-specific CD4 T cell dependent polyclonal B-cell activation upon persistent viral infection is short lived and extrafollicular. *Eur. J. Immunol.* 2020. **50**: 396-403.

32. **Boyer, O., Saadoun, D., Abriol, J., Dodille, M., Piette, J. C., Cacoub, P. and Klatzmann, D.**, $CD4^+CD25^+$ regulatory T-cell deficiency in patients with hepatitis C-mixed cryoglobulinemia vasculitis. *Blood.* 2004. **103**: 3428-3430.

33. **Pileri, P., Uematsu, Y., Campagnoli, S., Galli, G., Falugi, F., Petracca, R., Weiner, A. J.**, Binding of hepatitis C virus to CD81. *Science.* 1998. **282**: 938-941.

34. **Rosser, E. C. and Mauri, C.,** Regulatory B cells: origin, phenotype, and function. *Immunity.* 2015. **42**: 607-612.

35. **Weisberg, I. S. and Jacobson, I. M.**, A pangenotypic, single tablet regimen of sofosbuvir/velpatasvir for the treatment of chronic hepatitis C infection. *Expert. Opin. Pharmacother.* 2017. **18**: 535-543.

36. Liang, T. J. and Ghany, M. G., Current and future therapies for hepatitis C virus infection. *N. Engl. J. Med.* 2013. **368**: 1907-1917.

37. Raj, V. S., Hundie, G. B., Schurch, A. C., Smits, S. L., Pas, S. D., Le Pogam, S., Janssen, H. L. A. et al., Identification of HCV Resistant Variants against Direct Acting Antivirals in Plasma and Liver of Treatment Naive Patients. *Sci. Rep.* 2017. **7**: 4688.

38. Bian, W. X., Xie, Y., Wang, X. N., Xu, G. H., Fu, B. S., Li, S., Long, G. et al., Binding of cellular nucleolin with the viral core RNA G-quadruplex structure suppresses HCV replication. *Nucleic. Acids. Res.* 2019. **47**: 56-68.

39. Cossarizza, A., Chang, H. D., Radbruch, A., Acs, A., Adam, D., Adam-Klages, S., Agace, W. W. et al., Guidelines for the use of flow cytometry and cell sorting in immunological studies (second edition). *Eur. J. Immunol*. 2019. **49**: 1457-1973.

40. Yang, Y. F., Zhou, Y. D., Hu, J. C., Luo, F. L., Xie, Y., Shen, Y. Y., Bian, W. X. et al., Ficolin-A/2, acting as a new regulator of macrophage polarization, mediates the inflammatory response in experimental mouse colitis. *Immunology.* 2017. **151**: 433-450.

Figure legends

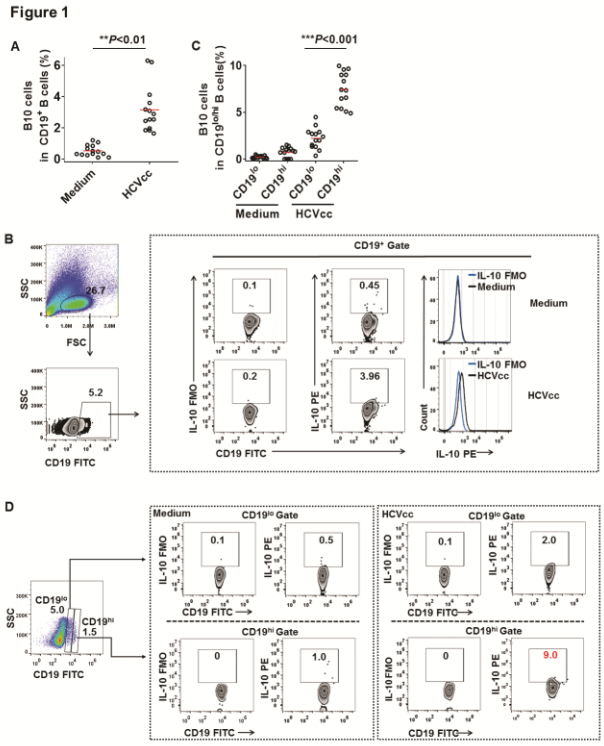

Figure 1. HCVcc induces B10 cells in human PBMC in vitro. (*A*) and (*B*) Human PBMCs were stimulated with HCVcc for 48 h, B10 cells were determined by flow cytometry. (*A*) Pooled data of the frequency of B10 cells . ***P*<0.01, ANOVA with Neuman-Keuls post hoc test. (*B*) Representative flow plots. (*C*) and (*D*) HCV-induced B10 cells were enriched in $CD19^{hi}$ B cells. (*C*) Pooled data of the frequency of B10 cells. ****P*<0.001, ANOVA with Neuman-Keuls post hoc test. (*D*) Representative flow plots. Data in (*A*) and (*C*) are shown as the mean ± SD (n=14 donors). The data are summary of three independent experiments using n = 14 donors in total.

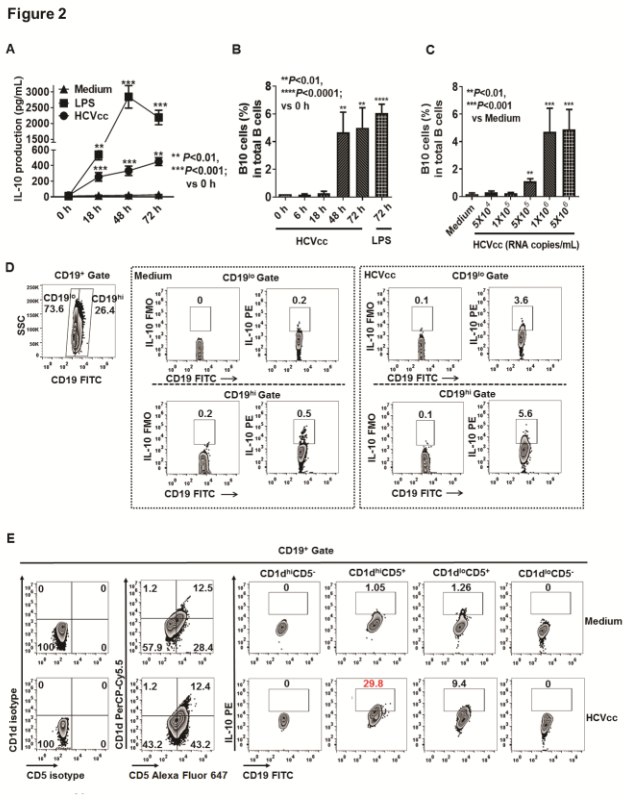

Figure 2. HCVcc induces murine B10 cells in vitro. (*A*) IL-10 production by B cells after HCVcc stimulation. Murine B cells were stimulated with HCVcc (1×10^6 RNA copies/mL) or LPS (10 μg/mL) for 0 h, 18 h, 48 h and 72 h. IL-10 production in cell culture supernatant was detected by ELISA. (*B*) Murine B cells were stimulated with HCVcc (1×10^6 RNA copies/mL) for the indicated time periods. B10 cell frequencies were determined by flow cytometry. (*C*) B cells were stimulated with various concentrations of HCVcc for 48 h, B10 cells were determined by flow cytometry. Data in (*A*) - (*C*) are shown as the mean ± SD (n=3 mice per experiment). ***P*<0.01, ****P*<0.001, *****P*<0.0001, ANOVA with Neuman-Keuls post hoc test. (*D*) and (*E*) B cells were stimulated with HCVcc (1×10^6 RNA copies/mL) for 48 h. B10 cell percentages were determined in $CD19^{hi/lo}$ B cells or $CD1d^{hi/lo}CD5^{+/-}$ B cells. All data are representative of at least three independent experiments with similar results.

Figure 3

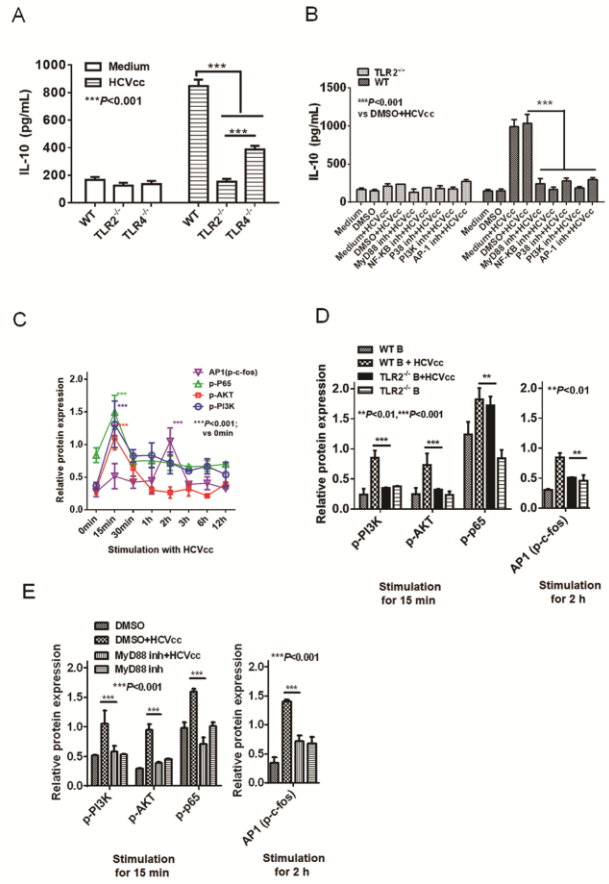

Figure 3. HCVcc induces IL-10 production by B cells via TLR2-MyD88-NF-κB and AP-1 signaling pathway. (*A*) Murine $CD19^+$ B cells were isolated from splenocytes of $TLR2^{-/-}$, $TLR4^{-/-}$ and WT mice. The B cells were stimulated with HCVcc for 48 h. The IL-10 concentrations in the supernatants were detected by ELISA. (*B*) Murine WT B cells were treated with MyD88, PI3K, P38, NF-κB and AP1 inhibitor for 1 h prior to stimulation with HCVcc. After 48 h of HCVcc stimulation, the concentration of IL-10 in culture supernatant was determined by ELISA. (*C*) WT B cells were stimulated with HCVcc for the indicated time periods. The phosphorylation of PI3K, AKT, NF-κB and AP1 were determined by immunoblot analysis. (*D*) WT B cells and $TLR2^{-/-}$ B cells were stimulated with HCVcc for the indicated time periods. The phosphorylation of PI3K, AKT, NF-κB and AP1 were determined by immunoblot analysis. (*E*) WT B cells were stimulated with HCVcc in the presence of MyD88 inhibitor for the indicated time periods. The phosphorylation of PI3K,

AKT, NF-κB and AP1 were then determined by immunoblot analysis. β-actin was used as a loading control (*C*-*E*). Data in (*A*)–(*E*) are shown as the mean ± SD (n=3 mice per experiment). ***P*<0.01, ****P*<0.001, ANOVA with Neuman-Keuls post hoc test. All Data are from a single experiment representative of at least three independent experiments.

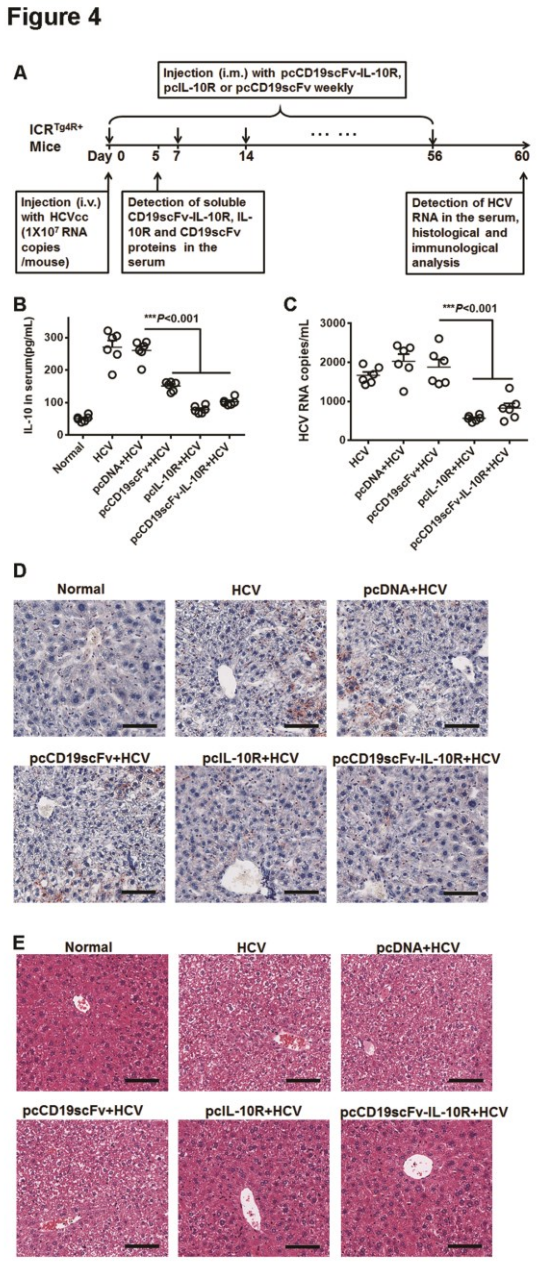

Figure 4. Neutralization of IL-10 secretion by B cells reduces viral loads during persistent HCV infection in humanized mice (*A*) Schematic diagram. On day 0, the ICR^{Tg4R+} mice were

infected with HCVcc (1×10^7 RNA copies/mouse, i.v.) and injected with pcCD19scFv-IL-10R, pcIL-10R or pCD19scFv once a week. On Day 60, the viral loads in the mice and anti-HCV immune response were assessed. (*B*) Serum IL-10 concentrations were determined by ELISA 60 dpi. (*C*) Serum HCV RNA copies were detected by RT-qPCR based on the relative expression of GAPDH. (*D*) IHC assay for NS3 detection in liver tissues (200X). Scale bars, 100 μm. (*E*) Liver specimen was stained with HE (200X). Scale bars, 100 μm. Data in (*B*)–(*C*) are shown as the mean ± SD (n=6 mice per experiment). ***P<0.001, ANOVA with Neuman-Keuls post hoc test. (D)-(E) Representative of three mice per experiment. All data are representative of at least three independent experiments with similar results.

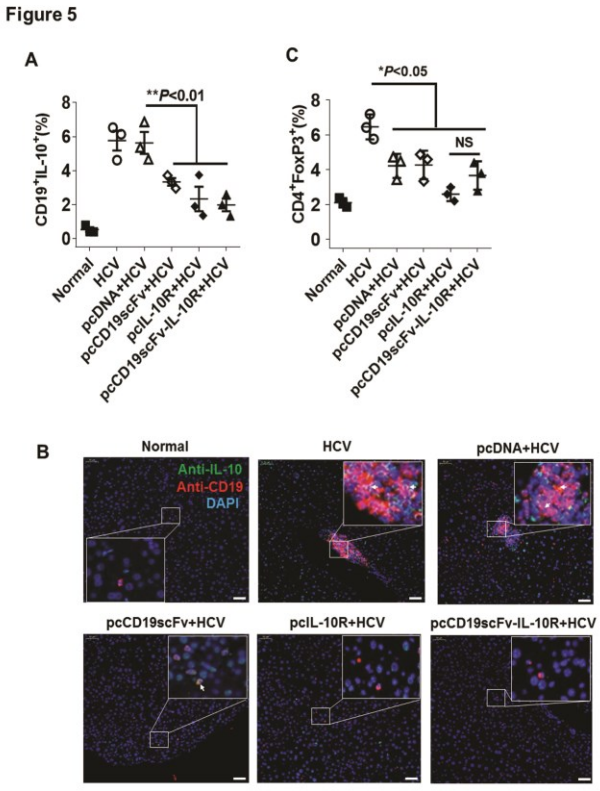

Figure 5. Blocking IL-10 production by B cells reduces B10 cells in HCV-infected mice. The HCV-infected mice were subjected to pcCD19scFv-IL-10R, pcCD19scFv or pcIL-10R treatment. (*A*) On Day 60, splenic B10 cells were determined by flow cytometry. (*B*) B10

cells in liver tissues were assessed by immunofluorescence assay (200X). Scale bar:100 μm. Smaller images on the sides were after ×3.3 magnification. (*C*) Splenic Treg cells were determined by flow cytometry. Data in (*A*) and (*C*) are shown as the mean ± SD (n=3 mice per experiment). **P*<0.05, ***P*<0.01, ANOVA with Neuman-Keuls post hoc test. All data are representative of at least three independent experiments with similar results.

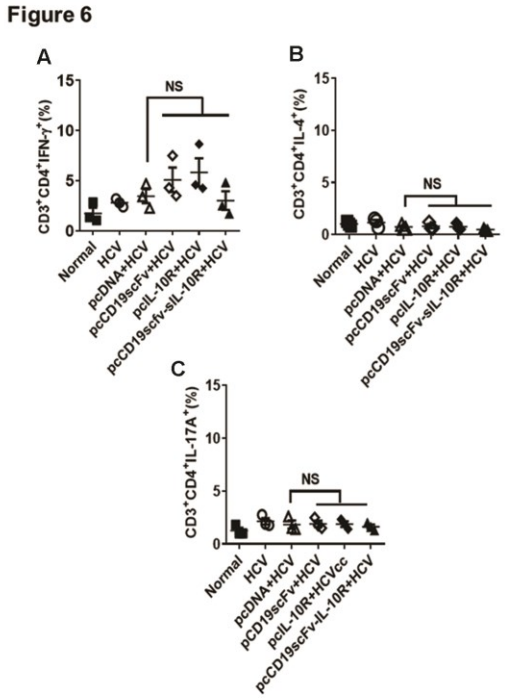

Figure 6. Neutralizing IL-10 production by B cells has no effect on Th polarization during HCV infection. The HCV-infected mice were subjected to pcCD19scFv-IL-10R, pcCD19scFv or pcIL-10R plasmid treatment. On Day 60, IFNγ$^+$ Th1 (*A*), IL-4$^+$ Th2 (*B*) and IL-17A$^+$ Th17 (*C*) cells were determined by flow cytometry. Data in (*A*)-(*C*) are shown as the mean ± SD (n=3 mice per experiment). NS, no significant (*P*>0.05), ANOVA with Neuman-Keuls post hoc test. All data are representative of at least three independent experiments with similar results.

Figure. 7

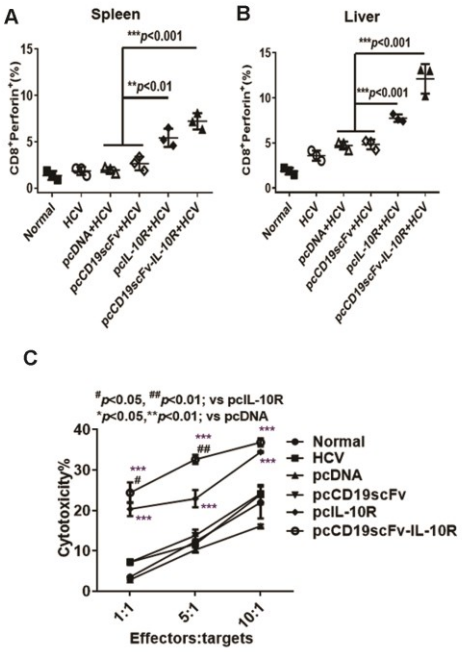

Figure 7. Neutralization of IL-10 production by B cells increases cytotoxic T cell activity in HCV-infected mice. The HCV-infected mice were treated with pcCD19scFv-IL-10R, pcCD19scFv or pcIL-10R plasmids. On Day 60, perforin^{+}CD8^{+} T cells from (*A*) spleen and (*B*) liver were determined by flow cytometry. Data are shown as the mean ± SD (n=3 mice per experiment). ***P*<0.01, ****P*<0.001, ANOVA with Neuman-Keuls post hoc test. (*C*) pcCD19scFv-IL-10R treatment leads to increased level of cytotoxic activity of the splenocytes. On Day 60, murine splenocytes were collected, stimulated with anti-CD3 mAb, anti-CD28 and IL-2 for 5 days and were used as effector cells. Hepatocytes from HCV-infected mice (HCV group) were used as target cells. The LDH release assay were performed for cytotoxicity. Representative data are shown as the mean ± SD (n=6 mice per experiment). **P*<0.05, ***P*<0.01, vs pcDNA group; $^{\#}$*P*<0.05, $^{\#\#}$*P*<0.01, vs IL-10R group; ANOVA with Neuman-Keuls post hoc test. All Data are from a single experiment representative of three independent experiments.